Case Studies in Chemical and Environmental Engineering 4 (2021) 100121

Contents lists available at ScienceDirect

Case Studies in Chemical and Environmental Engineering

journal homepage: www.sciencedirect.com/journal/case-studies-in-chemical-and-environmental-engineering

Functionalized cellulose nanocrystals as a novel adsorption material for removal of boron from water

ARTICLE INFO

Keywords
Cellulose nanocrystals
Adsorption
Boron
Groundwater
Case study

ABSTRACT

This study aims to prepare a novel adsorbent containing cellulose nanocrystals (CNC) isolated from date pits (DP) and ionic liquid (IL). The prepared composite of CNC and IL was then loaded onto the DP to prepare IL-CNC@DP adsorbent. The boron remediation capability was then investigated using the prepared adsorbent and compared to that of DP. The results showed the superior performance of IL-CNC@DP as compared to DP. The maximum adsorption capacity of 97 mg/g and 69 mg/g was obtained with IL-CNC@DP and DP, respectively. This can be attributed to the high surface area of 4.254 m^2/g for IL-CNC@DP as compared to 2.126 m^2/g for DP. The effect of pH, temperature, and initial boron concentration on adsorption was also studied. It was noticed that the % removal of boron from water increased with pH and reached its maximum of around 97% at pH 6. On the other hand, there was no effect of temperature (25 °C, 35 °C, and 45 °C) on adsorption capacity noted for both adsorbents. The results also indicated that the adsorption of boron from water by the prepared adsorbent favors the Dubinin-Radushkevich isotherm model.

1. Introduction

Groundwater makes around 98% of all the useable freshwater found on earth and it is around 60 times as abundant as the freshwater found in lakes and streams [1]. Due to the movement of groundwater through different rocks, soil, and geological formations, groundwater acquires a variety of elements, minerals, compounds, and pollutants causing deterioration in groundwater quality. There are several cases in which contamination of groundwater with toxic metals and microorganisms has been reported [2,3]. Qatar utilizes 92% of the groundwater resources for agricultural purposes [4], which has been found to be contaminated with boron at the concentration of 3.819 mg/L at some sites [2]. Due to the potential toxicity of boron to the health of plants and animals [5,6], there is a need to develop environment-friendly and technologically efficient techniques for the removal of boron from water, making it effective for reuse in agriculture.

Due to its low cost, feasibility, environment friendly, and simple operation, the adsorption technique has been employed for the treatment and removal of a variety of pollutants and metals from water [7]. To further improve the economic efficiency of the adsorption technique, there is an increased interest in utilizing and reusing biomass such as eggshells, rice husk, and banana peels to produce novel adsorbents. Recently, Rukayat et al. [8] used rubber leaves powder from rubber plants for the adsorptive removal of copper from water. The maximum adsorption capacity of 9.074 mg/g was obtained and it was found that the adsorption follows the physisorption mechanism. Date pits (the seeds of the date fruit) are one of the major constituents of solid waste in Qatar. Our previous research has also shown the adsorptive characteristics of modified date pits for the removal of metals, dyes, and other pollutants [9,10]. Therefore, in this research, the date pits were utilized for two purposes i.e. (1) as a source of cellulose and (2) as a support for the prepared adsorbent (Fig. 1).

Cellulose is a linear chain of anhydroglucose monomer units connected through 1–4 β-linkages. It contains both crystalline and amorphous regions. The structure, properties, and size of cellulose depend upon the source from where it is extracted [11]. Isolation of cellulose and preparation of cellulose nanocrystals occurs in two steps. In the first step (termed as pre-treatment), the isolation of cellulose from fruit fibers is done through chemical pretreatment [12]. The chemical pretreatment helps to remove lignin, hemicellulose, and extractives (lignans, flavonoids, and phenolics). Then bleaching is performed using chlorine dioxide, hydrogen peroxide, or sodium percarbonate to obtain a higher degree of whiteness and enhance the purity of cellulose [13].

To produce CNC from cellulose, the hydrolysis step is needed using a mineral acid under controlled conditions. The cellulose after the bleaching step contains some amorphous regions which are weak and sensitive to acid attack. Therefore, after the hydrolysis step, cellulose with a high level of crystallinity, needle-like structure, with high aspect ratio, and nano-size is obtained which is called cellulose nanocrystals (CNC) [14].

Due to the several useful features of ionic liquids (ILs), they have been shown to combine with nanomaterials for combined functionalities and their use has been demonstrated in electrochemistry, catalysis, and separations [15]. Recent research has shown the adsorptive removal of lithium from water using IL-based adsorbents [15] and membranes [16]. ILs provide better thermal stability, ionic conductivity, and good solubility for cellulose and contain a variety of functional groups which can help to dissolve cellulose [17] and provide a unique platform for its functionalization.

The cellulose and cellulose nanocrystals obtained and prepared from various agricultural products have been used for the treatment of water. In the current case study, the cellulose was extracted from date pits to produce cellulose nanocrystals (CNC), which were then modified with ionic liquid (IL) to produce IL-CNC. The nanocomposite was then

https://doi.org/10.1016/j.cscee.2021.100121
Received 16 July 2021; Received in revised form 10 August 2021; Accepted 11 August 2021
Available online 14 August 2021

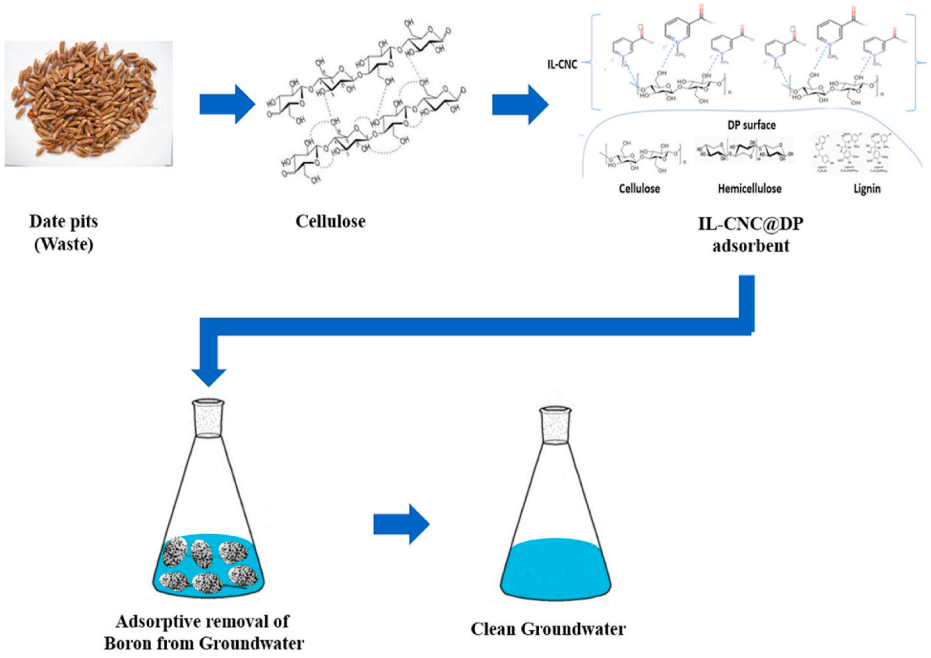

Fig. 1. Schematic illustration of biomass-derived adsorbent and adsorptive removal of boron from contaminated water.

deposited onto the powdered date pits (DP) to produce a novel adsorbent as IL-CNC@DP (Fig. 1). Thus, the prepared adsorbent (IL-CNC@DP) was then applied for the adsorptive removal of boron from water at different concentrations simulating a wide range of their concentrations in groundwaters (Fig. 1). The performance of the IL-CNC modified adsorbent was compared with date pits (DP), used as a control.

2. Experimental methods

2.1. Preparation of the modified IL-CNC@DP adsorbent

50 g of ground DP (0.125 mm - 0.250 mm) was delignified using 6.0% sodium hydroxide (Sigma Aldrich/USA) for 4 hours under 70 °C followed by washing until neutral pH was achieved. The bleaching of the mixture was done using 6.0% sodium hypochlorite (Sigma Aldrich/USA) followed by washing again to obtain neutral cellulose. After drying overnight, the pure cellulose was then subjected to acid hydrolysis using 64% sulfuric acid (Sigma Aldrich/USA) for 1 hour under 25 °C to obtain cellulose nanocrystals (CNC). The CNC was then washed thoroughly with distilled water and was separated by centrifugation at 5000 rpm for 0.5 hours. Finally, the CNC was soaked in pure distilled water by using a dialysis membrane (Fisher Scientific/USA), and the dialyzed suspension of the CNC was dispersed by ultrasonication at 600 w for 15 mins.

The next step involved ionic liquid (3-formyl-1-methyl pyridinium iodide, C_7H_8INO, MWt. 249.05 g/mol) to be solubilized in DMSO (dimethyl sulphoxide, Sigma Aldrich/USA) at 65 °C with constant mixing until the solution is homogenized. Then, the already extracted CNC was added to the mixture at 1:1 to produce an IL-CNC composite. Finally, 5 g of DP (0.125 mm - 0.250 mm) was mixed with the suspension of the prepared IL-CNC until homogenization was achieved. The resultant IL-CNC@DP was dried in the oven for 2 hours at 60 °C [18].

2.2. Characterization of the adsorbents (IL-CNC@DP and DP)

Both adsorbents (IL-CNC@DP and DP) were characterized using a variety of techniques. A scanning electron microscope (SEM) (JEOL model JSM-6390LV) was used to evaluate the morphological characteristics of the adsorbent's surface. The functional groups of the adsorbents were studied using Fourier transform infrared (FTIR) (RSpirit-T model). Furthermore, the surface areas of the prepared materials were characterized using the Brunauer, Emmett, and Teller (BET) (Aim Sizer-AM301). The results were obtained by nitrogen adsorption measurements that are made at liquid nitrogen temperature, 77 K. Lastly, a zeta potential test was conducted to study the surface charge of both adsorbents in water liquid suspension at 25 °C using Zetasizer Nano ZS (Malvern Instruments) [18].

2.3. Preparation of boron stock solution and batch adsorption studies

A boron stock of 100 ppm was prepared by adding 0.572 g of H_3BO_3 (Sigma Aldrich/USA) in a 1 L volumetric flask with distilled water. The effect of different parameters on the adsorption of boron was studied. Initially, to investigate the optimum conditions for adsorption, the experiments were carried out at different pH values (2, 4, 6, 8, and 10) randomly selected to cover acidic, alkaline, and neutral conditions. Once, the optimum pH for adsorption was known for both adsorbents, the experiments were carried out at different initial concentrations of boron and different temperatures simulating the real groundwater conditions. Thus, the experiments were carried out at the initial concentration of boron (5, 10, 15, 20, 25, 30, 35, 50, 70, and 100 mg/L) and temperature (25 °C, 35 °C, and 45 °C). Each experiment was conducted in duplicates and the mean values and standard errors were calculated.

Briefly, the 1:1 ratio of the adsorbent mass (0.05 g) and volume (50 mL) of the solution were used in glass bottles and placed in the shaker for 24 hours at 165 rpm. After each test, the spent adsorbents were filtered through a 0.2 μm syringe filter and were air-dried for further analysis using SEM and FTIR. Duplicates and blanks were used in each experiment. The initial and equilibrium boron concentrations were analyzed by using inductively coupled plasma - optical emission spectrometry (ICP-OES) (an IRIS Intrepid by ThermoFisher Scientific). The percentage of solute removal was calculated as per equation (1) [11].

$$Removal\ (\%) = \left[\frac{C0 - Ce}{C0}\right] \times 100 \quad (1)$$

Where C_0 and C_e are the initial and equilibrium boron concentrations (mg/L), respectively.

Moreover, the adsorption capacity was calculated as per equation (2).

$$qe = [C_0 - Ce]X\frac{V}{M} \quad (2)$$

Where C_0 and C_e are the initial and equilibrium boron concentrations (mg/L), respectively, V is the volume (L), and M is the weight of the adsorbent (g).

2.4. Thermodynamic studies of boron adsorption onto IL-CNC@DP and DP

The three thermodynamic parameters (ΔG°, ΔH°, and ΔS°) were calculated as per equations (3) and (4) [7].

$$\Delta G^\circ = -RT\ln K_L \quad (3)$$

Where R is the universal constant 8.314 J/mol.K, T corresponds to the

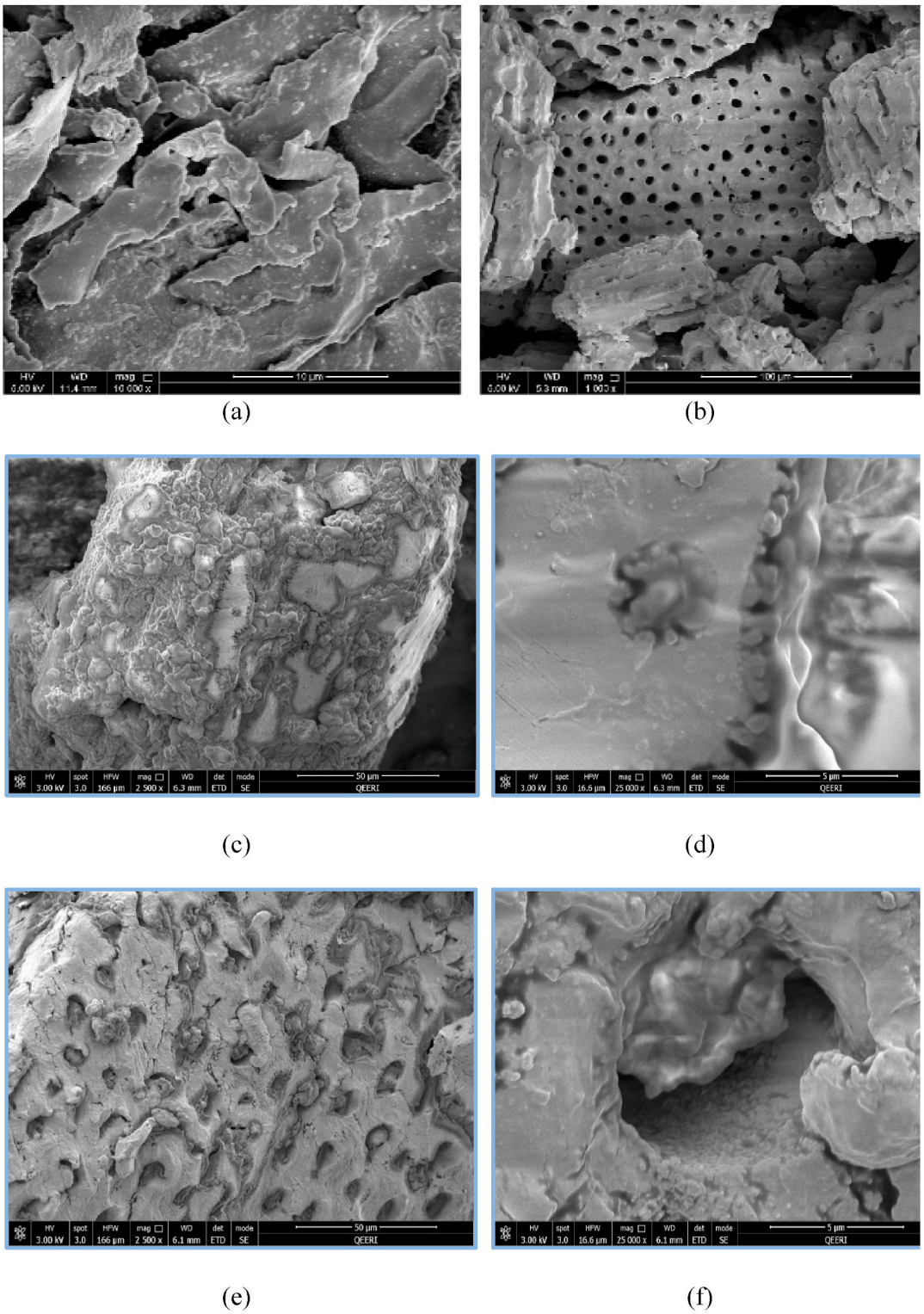

Fig. 2. Surface morphological analysis through SEM (a, b) CNC; (c, d) DP; (e, f) IL-CNC@DP

temperature measured in Kelvin, and K_L represents the Langmuir isotherm constant. Temperature is used to express the standard enthalpy and entropy changes of adsorption.

$$\ln K_L = -\frac{\Delta H^o}{RT} + \frac{\Delta S^\circ}{R} \quad (4)$$

Where ΔH° and ΔS° are determined from the slope and intercept of the equation of the line, which is evaluated from the plot of $\ln K_L$ vs. 1/T.

Four isotherm models were used in this study to determine the best-fit model for the adsorption process: Langmuir, Freundlich, Dubinin-Radushkevich, and Temkin isotherm models.

2.5. Desorption studies

The desorption was carried out for a total of 0.05 g of spent IL-CNC@DP and DP. The spent adsorbents were tested under two different solutions: 0.5 M HCl, and 1 M HCl. The supernatant was then analyzed by ICP-OES (an IRIS Intrepid by ThermoFisher Scientific). Duplicates and blanks were used in each experiment. The desorption percentage was calculated according to equation (5) [7].

$$Desorption\ (\%) = \left[\frac{C0 - Ce}{C0}\right] \times 100 \quad (5)$$

Where C_0 and C_e are the average adsorption and desorption concentrations (mg/L), respectively.

3. Results and discussion

3.1. Characterization of IL-CNC@DP and DP

3.1.1. Surface morphology and functional group analysis

The SEM and FTIR techniques were used to analyze the surface morphology and the presence of different functional groups on the adsorbents (IL-CNC@DP and DP) [18]. Fig. 2 shows the SEM images of the CNC and the two adsorbents. In Fig. 2a and b, the CNC appeared as microfibril structures that are highly packed due to the hydrogen bonding between them. It is evident from Fig. 2c and d that the DP possessed a smooth surface, while pores and cavities are not much apparent. In comparison, the prepared adsorbent (IL-CNC@DP) in Fig. 2e and f shows a porous surface with abundant cavities and sites for the potential adsorption of pollutants.

The FTIR spectra of CNC and the two adsorbents are provided in Fig. 3. From Fig. 3a, the functional groups of cellulose corresponding to C–O–C deformation and stretching can be seen at 790 cm^{-1}. Moreover, the stretching vibration of the C–O–C bonds representing the cellulose 4-glycosidic linkages of the D-glucose units can also be seen at peaks 1162 cm^{-1} and 1034 cm^{-1} [19]. The DP mainly comprises cellulose, hemicellulose, and lignin. Different functional groups of DP components can be seen from the FTIR spectra depicted in Fig. 3b. The broadband centered around 3300 cm^{-1} can be attributed to the free or inter/intra-molecular bonded hydroxyl (-OH) groups present in the cellulose component of DP. In the fingerprint region of 1800 cm^{-1} – 600 cm^{-1}, there are various well-defined peaks such as the presence of a sharp peak at 1744 cm^{-1} which can be attributed to the unconjugated C═O of hemicellulose. Similarly, peaks around 1375 cm^{-1}, 1320 cm^{-1}, 1058 cm^{-1}, and 869 cm^{-1} can be attributed to the C–H deformation, C–H vibration, C–O stretching, and C–H deformation of cellulose and hemicellulose, respectively [20]. Moreover, a peak at 1246 cm^{-1} for C–O stretching from lignin is also evident. The presence of IL can be observed between the 2900 cm^{-1} – 3300 cm^{-1} range as the broad peak became more complex and there is an appearance of additional peaks at 3348 cm^{-1} and 3445 cm^{-1}. The observed change in the peaks could have resulted from N–H stretching vibration [21] from IL (3-formyl-1-methyl pyridinium iodide) incorporated in IL-CNC@DP adsorbent [10].

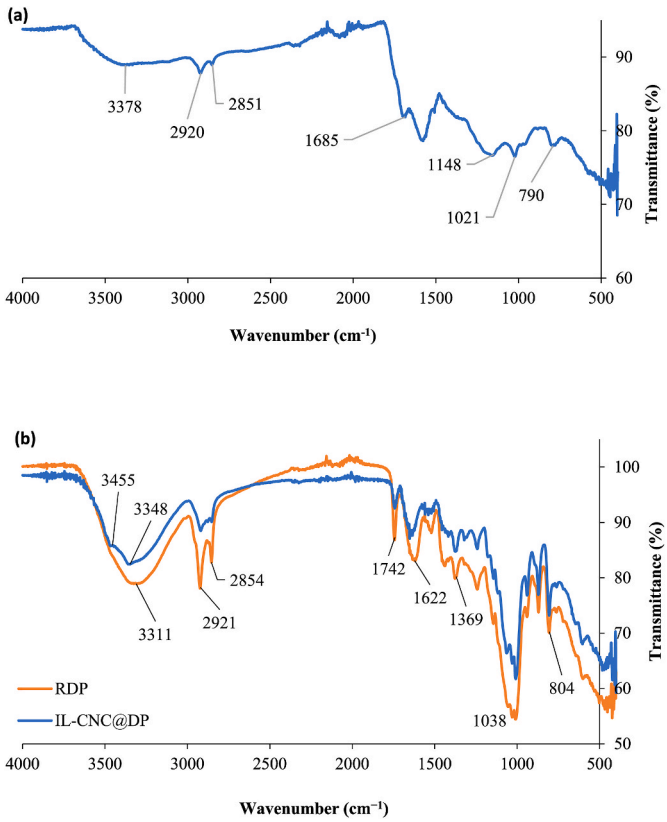

Fig. 3. FTIR graphs of (a) CNC and (b) DP and IL-CNC@DP.

3.1.2. Surface charge, surface area, and porosity measurements

The surface charge of the adsorbents was measured through zeta potential measurements. The results showed that the surface charge is equal to −28.85 mV and −27.76 mV for IL-CNC@DP and DP, respectively (Table 1). The negative values show that the charges in the interface between the adsorbent and solution that contains boron ions are negative, thus establishing electrostatic attraction forces that support the adsorption process. However, the zeta potential values for IL-CNC@DP are slightly more negative than the zeta potential values for DP. This means that IL-CNC@DP is more stable in the adsorption solution than DP and more electrostatically negative, which presents more electrostatic attraction forces towards the positively charged boron ions.

The specific surface area and pore volume of the adsorbents were measured using nitrogen adsorption-desorption measurements using the BET method (Fig. 4). The results showed that the DP adsorbent had a specific surface area of 2.126 m^2/g with a pore volume of 0.008611 cm^3/g, while the specific surface area of the IL-CNC@DP adsorbent was found to be higher than the DP i.e., 4.254 m^2/g with a pore volume of 0.015527 cm^3/g (Table 1). Thus, high porosity, more surface area, and rough surface shown by BET measurement and SEM analysis for IL-CNC@DP adsorbent demonstrate the potential of prepared adsorbent for removal of boron from water [10].

3.2. Boron adsorption experiments

3.2.1. Effect of pH

Fig. 5a demonstrates the percentage removal of boron by the IL-CNC@DP and DP. It can be concluded that the increase in the pH value demonstrates an increase in the % removal of boron by both adsorbents, IL-CNC@DP and DP. The lowest adsorption is shown at pH 2, as only 77% removal efficiency was observed. The highest percentage removal of 98% was achieved at pH 6, 8, and 10. Similar results were also reported by Al-Ghouti and Salih [22], where the maximum

Table 1
Summary of the surface charge and area of both adsorbents.

Adsorbent	Average Zeta Potential (mV)	Specific surface area (m^2/g)	Pore volume (cm^3/g)
DP	−28.54	2.126	0.008611
IL-CNC@DP	−27.76	4.254	0.015527

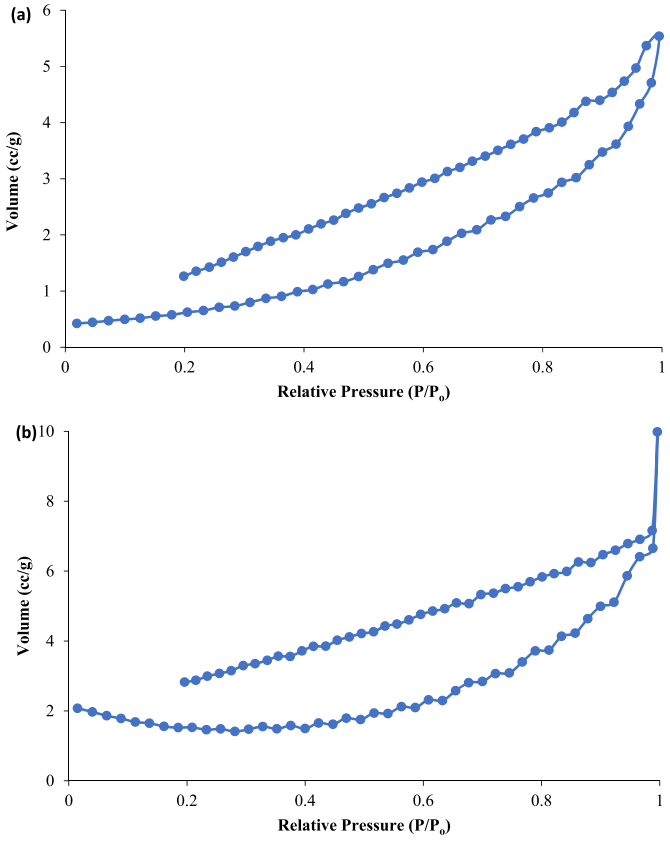

Fig. 4. Nitrogen adsorption-desorption curves for (a) DP and (b) IL-CNC@DP

adsorption of boron occurred at pH 6. Generally, at high pH, the high number of hydroxyl ions present can cause the precipitation of metals in the hydroxide forms as well as cause the electrostatic repulsion due to the presence of the same ion charges in the aqueous solution [22]. Nonetheless, in this experiment, boron was present mainly as a boric acid solution i.e. $(BO_3)^{3-}$ or $B(OH)^{4-}$. Therefore, it can be deduced that the adsorptive removal of boron occurs due to the hydrogen bonding between the hydroxyl groups of cellulose and boric acid [23].

Hossain et al. [20], investigated the removal of boron from aqueous medium by date pits and obtained a removal efficiency of 71% at a neutral pH value. Similarly, another study conducted by Ahmed et al. [5], found that at neutral pH, the removal efficiency of date pits reached 89%. Al-Haddabi et al. [4], found a lower removal capacity of boron at neutral pH in which their results showed that date pits are capable of removing only 47% of boron from water.

The concept of "faked" adsorption should be considered when studying the effect of pH since at more basic pH values more OH^- ions are found in the solution, which will encourage hydroxide precipitation of boron metals [24]. Therefore, adsorptive removal of boron was not considered at higher pH. As for the control adsorbent (DP), the removal capacity was much less in comparison to the prepared adsorbent demonstrating the capability of IL-CNC for boron adsorption.

Consequently, according to the obtained results for boron removal, the best pH value of 6 was selected for IL-CNC@DP adsorbent. As for DP, even though a pH value of 10 demonstrates the highest removal efficiency, the pH value of 4 was selected since there was a slight difference between %removal obtained at pH 4, 6, and 8. This can also discard the concept of "faked" adsorption that comes into play at higher pH values.

3.2.2. *Effect of initial boron concentration*

Fig. 5b demonstrates the adsorption capacity for boron onto the IL-CNC@DP (pH 6) and DP (pH 4) investigated at different initial concentrations. It is evident that there is a steady increase in adsorption capacity along with the increase in boron concentrations for both adsorbents. Moreover, the adsorption capacity of the prepared novel adsorbent (IL-CNC@DP) was significantly higher than that of DP. At high concentration, it is expected that the increase in the collision between the boron and the adsorbents resulted in enhanced mass transfer between them and subsequent uptake of boron from water by the adsorbent [18].

In this study, the highest adsorption capacity is at 100 mg/L for IL-CNC@DP as it reached 97 mg/g with 97% adsorption efficiency. It is probable that the adsorbent will eventually reach a plateau as the limited available sites are used. In comparison with the literature, so far the highest adsorption capacity for boron was found to be 145.5 mg/g under optimum conditions using glucamine-functionalized hydrogel beads [25]. Nevertheless, the unmodified adsorbent reaches its all-time high at 65 mg/g at 100 mg/L; therefore, boron can still be remediated from the environment using the DP.

3.2.3. *Effect of temperature*

From Fig. 5c, the reaction under 25 °C, 35 °C, and 45 °C can be compared and it is evident that the amount of boron adsorbed by IL-CNC@DP is not significantly different amongst each other. Therefore, this study indicates that the effect of the three temperatures was not a significant factor for the prepared adsorbent. The results demonstrate the adsorption capacity of boron at 5 mg/L onto IL-CNC@DP to be 4.50 mg/g (90.1%) at 25 °C then to increase slightly to 4.64 mg/g (92.9%) at 35 °C and then to decrease to 4.04 mg/g (80.9%) at 45 °C. Comparing these results to the adsorption capacity of boron at 100 mg/L, it was found to be 89.4 mg/g (97.60%) at 25 °C then to increase slightly to 98.2 mg/g (98.25%) at 35 °C and finally to 99 mg/g (99.00%) at 45 °C. Consequently, this shows the availability of active sites on the surface of the adsorbent at increasing initial concentrations. This can further prove that the removal of boron by the adsorption process using modified IL-CNC@DP adsorbent can be effective at low temperatures (25 °C) since it shows high adsorption capacities at high initial concentrations. Despite that recent findings validate that the effect of the temperature factor does in fact contribute to the adsorption capacity [10,22,26]. In this study, the temperature factor did not play a significant role in the modified adsorbent.

The other adsorbent, DP, illustrated in Fig. 5d presents an increase of boron adsorption with increasing initial concentrations, but with more obvious variations under the three different temperatures. Additionally, the adsorption capacity of boron at 5 mg/L onto DP was found to decrease from 0.44 mg/g (8.80%) at 25 °C to 0.32 mg/g (6.40%) at 35 °C and then increase to 0.40 mg/g (8.10%) at 45 °C. Therefore, in this study, at 100 mg/L, the optimum temperature was found to be 45 °C, where the highest adsorption capacity occurs onto DP.

For the wide range of boron initial concentrations studied in the literature (2 mg/L – 1000 mg/L), various other adsorbents have also shown to be effective in the removal of boron from water. The adsorption capacities have been found to be in the range of 1.5 mg/g – 145.5

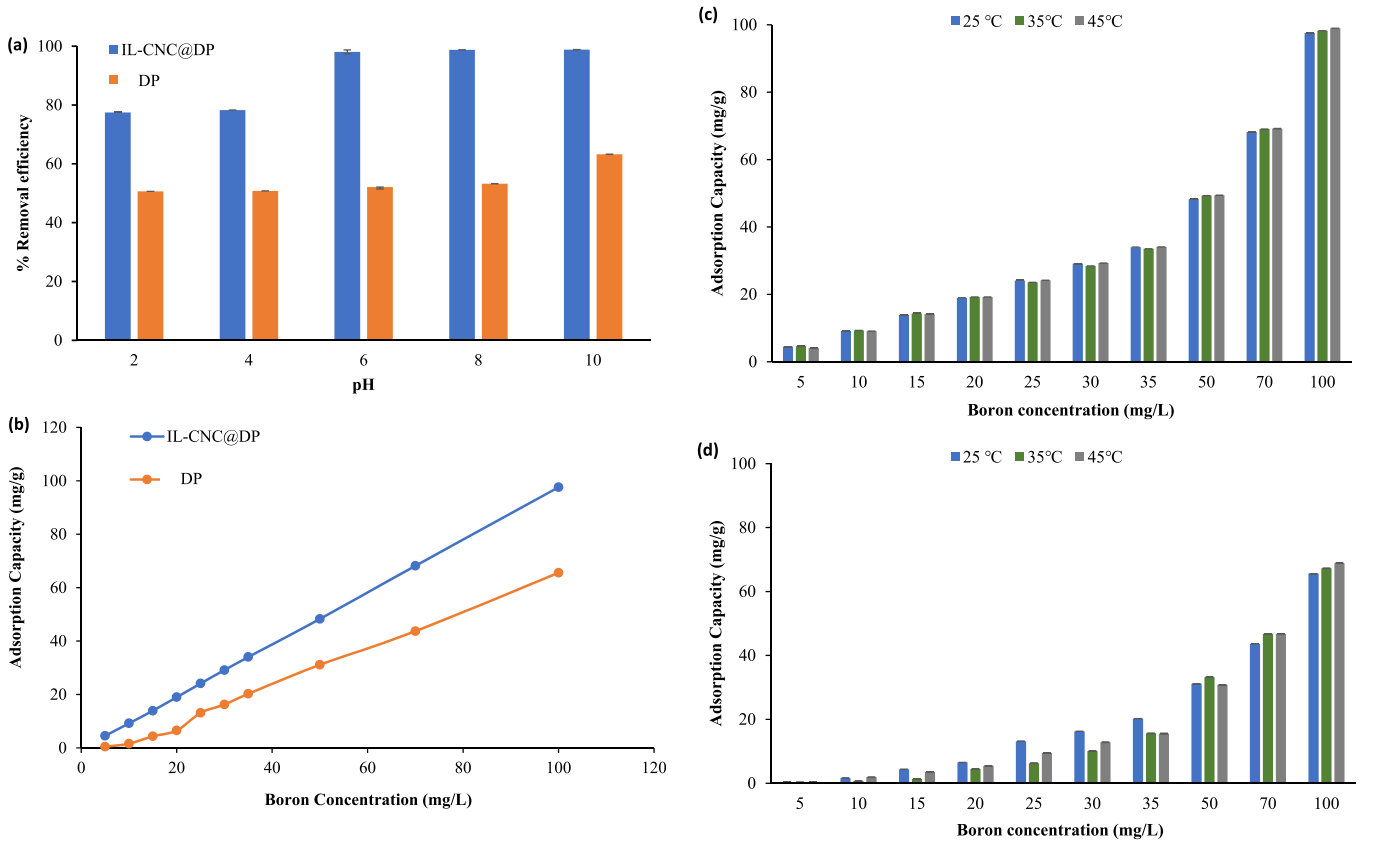

Fig. 5. Adsorption of boron in water (a) Effect of pH on %removal efficiency of boron by IL-CNC@DP and DP (initial boron concentration = 100 mg/L, Temperature = 25 °C); (b) Effect of boron initial concentration on adsorption capacities of both adsorbents (pH for DP = 4, for IL-CNC@DP = 6, Temperature = 25 °C); (c) Effect of temperature on adsorption capacity of IL-CNC@DP (pH = 6); and (d) Effect of temperature on adsorption capacity of DP (pH = 4).

mg/g [4,5,25,27–32] (Table 2). Whereas, in this research, the highest adsorption capacity of 97 mg/g for the prepared adsorbent was obtained for the maximum concentration of 100 mg/L, which showed its superior properties for adsorptive removal of boron from water.

3.3. Thermodynamic study of both adsorbents

The calculation of the thermodynamics was based on the previously mentioned Equations (3) and (4). In Table 3, the values of ΔG° are negative, indicating that the adsorption of boron onto IL-CNC@DP and DP is feasible, spontaneous, and does not need an external driving force for the reaction to take place. Similarly, the negative value of ΔH° indicates that the reactions were exothermic. Whereas the negative value of ΔS° confirmed that the adsorption of boron on the surface of the IL-CNC@DP and DP adsorbent is an associated mechanism and it does not favor the high level of disorder in the adsorption process. Recent findings also demonstrate that boron adsorption is most likely to be an exothermic and spontaneous process under favorable conditions [33–35].

Table 2
Comparison of adsorption capacities reported for removal of boron from water.

Adsorbent	Adsorption capacity (mg/g)	Reference
Bentonite and magnesite composite	99.8	[27]
Calcined alunite	49	[28]
Chitosan with nickel (II) hydroxide	61.4	[29]
Chitosan bead	70	[30]
Calcium alginate gel	94	[31]
Date pits	71	[20]
Date pits	89	[5]
Date palm seed ash	47	[4]
NMDG@cellulose fiber	18.5	[32]
Glucamine-functionalized hydrogel beads	145.5	[25]
Date pits	65[a]	This study
IL-CNC@DP	97[a]	This study

*NMDG: N-methyl-D-glucamine functional group.
[a] Obtained from Fig. 5b.

Table 3
Thermodynamic parameters for boron adsorption onto IL-CNC@DP & DP.

Adsorbent	ΔG° (kJ/mol)	ΔH° (kJ/mol)	ΔS° (kJ/mol.K)
IL-CNC@DP	−4037	−24942	−70.11
DP	−14.23	−117.73	−0.34

3.4. Isotherm study of both adsorbents

The isotherm parameters and constants obtained are shown in Table 4 for boron adsorption onto IL-CNC@DP and DP. From Table 4, it is evident that the R^2 values of the four isotherm models studied are different for the two adsorbents. As the R^2 values are low for some models, this means that the adsorption of boron onto both adsorbents might not follow all the studied models.

The value of R^2 for the Langmuir model of the IL-CNC@DP is low (0.75), therefore we can conclude that they do not follow the model's theory. On the other hand, the R^2 value (0.82) for DP shows that the boron adsorption follows the Langmuir model. This proves that the boron molecules form a homogenous monolayer on the surface of the DP adsorbent better than IL-CNC@DP. Regardless of the R^2 value, the monolayer adsorption capacity (Q_0) of IL-CNC@DP is much higher than

Table 4
The parameters of the two isotherms models for boron adsorption onto IL-CNC@DP and DP at 25 °C.

	Langmuir			Freundlich				Temkin			Dubinin-Radushkevich		
	Q_0 (mg/g)	b (L/mg)	R^2	K_f (mg/g) $(L/g)^n$	N	1/n	R^2	A_T (L/mg)	B (J/mol)	R^2	q_s (mg/g)	B_D	R^2
DP	4.72	297.36	**0.82**	102.4×10^5	0.16	6.1	**0.9**	2.51	120.93	**0.91**	68.46	-6×10^{-5}	**0.92**
IL-CNC@DP	588.2	980392	**0.75**	122	0.42	2.3	**0.81**	2.1	56.77	**0.8**	105.44	-5×10^{-7}	**0.93**

the DP adsorbent with values of 588.2 mg/g and 4.72 mg/g, respectively at 25 °C. Furthermore, the b constant values indicate the adsorbent and adsorbate affinity, and their values demonstrate the presence of strong binding of boron onto both adsorbents. Therefore, based on the Langmuir isotherm model the adsorption of boron onto IL-CNC@DP is followed to a certain degree but it is more favorable towards DP according to the R^2 value.

The Freundlich isotherm model was also studied for both adsorbents, and it presents high R^2 values (0.9) for the DP adsorbent as compared to IL-CNC@DP (0.81), which could mean that the studied adsorbent forms non-uniform multilayers on the DP surface. As well, the value of n for the two adsorbents was calculated to be less than 1 showing the chemical adsorption of boron onto the studied adsorbents. Another constant, which is 1/n, is found to be greater than 1 for both adsorbents, therefore this specifies a cooperative adsorption process. Lastly, the Freundlich constant (K_f) at 25 °C shows a high adsorption capacity of 122 mg/g for IL-CNC@DP and an extremely high adsorption capacity of 102.4×10^5 mg/g for DP.

The results of the Temkin adsorption isotherm model show high R^2 values for the DP (0.91) more than the IL-CNC@DP (0.8). Moreover, Temkin's heat of sorption constant (B) offers a chemical exothermic adsorption process of boron with higher values for the DP adsorbent. Hence, it can be concluded that this model is a better fit for DP in contrast to IL-CNC@DP at 25 °C.

The isotherm model of Dubinin–Radushkevich was also investigated. It was noted that the IL-CNC@DP and DP adsorbents have the highest R^2 values for the Dubinin–Radushkevich model at 25 °C, which shows that the adsorption process can be described as the best way through this model. The B_D values obtained for both adsorbents demonstrate that the adsorption process of boron is an energy-free process. Moreover, the adsorption capacity (q_s) values demonstrate that the IL-CNC@DP adsorbent can achieve higher adsorption of boron at 105.44 mg/g more than the DP, which can achieve 68.46 mg/g.

3.5. Desorption study

The desorption of the spent adsorbents and their reuse potential were also investigated using 0.5 M and 1 M HCl. The results showed that the removal of boron occurred mainly through the process of chemical adsorption and the binding of boron on the adsorbents was very strong as the desorption efficiency obtained was nearly zero [36]. This also means that the adsorbent cannot be effectively reused again. However, this can also imply that the type of eluent used for the desorption was not effective towards boron. Other eluents that could be employed in the desorption experiment towards boron can include H_2SO_4, HNO_3, EDTA, and thiourea [37]. These eluents are reported to be noteworthy in the recovery of metals, hence future experiments can be performed using these eluents for the desorption of boron.

4. Conclusion

In this research, biomass sourced cellulose was used to prepare IL-CNC composites which were then deposited on DP to produce IL-CNC@DP composite adsorbent. The characterization of the prepared adsorbent using a variety of techniques helped to obtain information on surface morphology, functional groups, porosity, and surface area of the adsorbents. The groundwater of Qatar has been shown to be contaminated with boron, which when used for irrigation could affect the health of plants and their consumers. Therefore, the prepared adsorbent was evaluated for its ability to remove boron from water. The results showed that boron from groundwater could be effectively remediated with high percentage removal efficiencies by using the IL-CNC@DP. The effect of pH, initial concentration, and the temperature had an impact on the adsorption of boron. The highest adsorption capacity of 97 mg/g for the IL-CNC@DP adsorbent was obtained at a temperature of 25 °C, pH 6, and an initial concentration of 100 mg/L boron. Furthermore, the thermodynamics constants of the modified adsorbent proved that the reaction is exothermic, does not favor a high level of disorder, and is spontaneous in nature. Langmuir, Freundlich, Dubinin–Radushkevich, and Temkin isotherm models were successfully used to find the best-fit model. Moreover, the desorption study demonstrated that boron cannot be desorbed from the used adsorbents. Therefore, further work is guaranteed to evaluate other eluents for desorption of boron from IL-CNC@DP. In addition, novel adsorbents will also be evaluated for simultaneous removal of multiple metals from the real groundwater of Qatar.

Declaration of competing interest

The authors declare that they have no known competing financial interests or personal relationships that could have appeared to influence the work reported in this paper.

Acknowledgment

This publication was made possible by NPRP grant # [12S-0307-190250] from the Qatar National Research Fund (a member of Qatar Foundation). The findings achieved herein are solely the responsibility of the author[s].

References

[1] K. Mullen, Information on Earth's Water, 2021. Retrieved from, https://www.ngwa.org/what-is-groundwater/About-groundwater/information-on-earths water.
[2] D.A. Da'ana, N. Zouari, M.Y. Ashfaq, M. Abu-Dieyeh, M. Khraisheh, Y.M. Hijji, M. A. Al-Ghouti, Removal of toxic elements and microbial contaminants from groundwater using low-cost treatment options, Curr. Pollut. Rep. (2021), https://doi.org/10.1007/s40726-021-00187-3.
[3] A.Y. Ahmad, M.A. Al-Ghouti, M. Khraisheh, N. Zouari, Hydrogeochemical characterization and quality evaluation of groundwater suitability for domestic and agricultural uses in the state of Qatar, Groundw. Sustain. Dev. 11 (2020) 100467.
[4] M. Al-Haddabi, M. Ahmed, Z. Al-Jebri, H. Vuthaluru, H. Znad, M. Al-Kindi, Boron removal from seawater using date palm (*Phonix dactylifera*) seed ash, Desalin. Waterr Treat. 57 (11) (2015) 1–8.
[5] M.M. Ahmed, M.S. Jami, M.E. Mirghani, M.N. Salleh, Investigation of the use of date seed for removal of boron from seawater, Bio. Natural Res. Eng. J. 3 (2) (2020) 55–73.
[6] M.Y. Ashfaq, M.A. Al-Ghouti, H. Qiblawey, N. Zouari, D.F. Rodrigues, Y. Hu, Use of DPSIR framework to analyze water resources in Qatar and overview of reverse osmosis as an environment friendly technology, Environ. Prog. Sustain. Energy 38 (4) (2018), https://doi.org/10.1002/ep.13081.
[7] E. Babiker, M.A. Al-Ghouti, N. Zouari, G. McKay, Removal of boron from water using adsorbents derived from waste tire rubber, J. Environ. Chem. Eng. 7 (2019) 102948.
[8] O.O. Rukayat, M.F. Usman, O.M. Elizabeth, O.O. Abosede, I.U. Faith, Kinetic adsorption of heavy metal (copper) on rubber (hevea brasiliensis) leaf powder, S. Afr. J. Chem. Eng. 37 (2021) 74–80.
[9] T. Shi, J. Ma, X. Wu, F. Wu, Inventories of heavy metal inputs and outputs to and from agricultural soils: a review, Ecotoxicol. Environ. Saf. 164 (2018) 118–124.

[10] M.A. Al-Ghouti, R.S. Al-Absi, Mechanistic understanding of the adsorption and thermodynamic aspects of cationic methylene blue dye onto cellulosic olive stones biomass from wastewater, Sci. Rep. 10 (1) (2020) 1–18.
[11] N. Razali, M.S. Hossain, O.A. Taiwo, M.I. Nadzri, N. Razak, N.M. Rawi, M. M. Mahadar, M.M. Kassim, Influence of acid hydrolysis reaction time on the isolation of cellulose nanowhiskers from oil palm empty fruit bunch microcrystalline cellulose, BioResour 12 (3) (2017) 6773–6788.
[12] L.Y. Ng, T.J. Wong, C.Y. Ng, C.M. Amelia, A review on cellulose nanocrystals production and characterization methods from Elaeis guineensis empty fruit bunches, Arab. J. Chem. 14 (9) (2021).
[13] T. Taflick, L.A. Schwendler, S.L. Rosa, C.D. Bica, S.B. Nachtigall, Cellulose nanocrystals from acacia bark–Influence ofsolvent extraction, Int. J. Biol. Macromol. 101 (2017) 553–561.
[14] M. El Achaby, Z. Kassab, A. Barakat, A. Aboulkas, Alfafibers as viable sustainable source for cellulose nanocrystalsextraction: application for improving the tensile properties ofbiopolymer nanocomposite films, Ind. Crop. Prod. 112 (2018) 499–510.
[15] S.A. Wahib, D.A. Da'na, N. Zaouri, Y.M. Hijji, M.A. Al-Ghouti, Adsorption and recovery of lithium ions from groundwater using date pits impregnated with cellulose nanocrystals and ionic liquid, J. Hazard Mater. 421 (2022).
[16] G. Zante, M. Boltoeva, A. Masmoudi, R. Barillon, D. Trébouet, Lithium extraction from complex aqueous solutions using supported ionic liquid membranes, J. Membr. Sci. 580 (2019) 62–76.
[17] Z. Li, A. Taubert, Cellulose/gold nanocrystal hybrids via an ionic liquid/aqueous precipitation route, Molecules 14 (11) (2009) 4682–4688.
[18] M.A. Al-Ghouti, Z.A. Al Disi, N. Al-Kaabi, M. Khraisheh, Mechanistic insights into the remediation of bromide ions from desalinated water using roasted date pits, Chem. Eng. J. 308 (2017) 463–475.
[19] D. Zheng, Y. Zhang, Y. Guo, J. Yue, Isolation and characterization of nanocellulose with a novel shape from walnut (Juglans Regia L.) shell agricultural waste, Polym. J. 11 (7) (2019) 1130.
[20] M.Z. Hossain, M.I. Waly, V. Singh, V. Sequeira, M.S. Rahman, Chemical composition of date-pits and its potential for developing value-added product- a review, Pol. J. Food Nutr. Sci. 64 (4) (2014) 215–226.
[21] S.A. Wahib, D.A. Da'na, N. Zaouri, Y.M. Hijji, M.A. Al-Ghouti, Mechanistic understanding of lithium ion adsorption from groundwater using modified date pits with cellulose nanocrystals and ionic liquid, J. Hazard Mater. (2021).
[22] M.A. Al-Ghouti, N.R. Salih, Application of eggshell wastes for boron remediation from water, J. Mol. Liq. 256 (2018) 599–610.
[23] J.-Y. Lin, N.N.N. Mahasti, Y.-H. Huang, Recent advances in adsorption and coagulation for boron removal from wastewater: a comprehensive review, J. Hazard Mater. 407 (2021) 124401.
[24] M.S. Anantha, S. Olivera, C. Hu, B.K. Jayanna, N. Reddy, K. Venkatesh, R. Naidu, Comparison of the photocatalytic, adsorption and electrochemical methods for the removal of cationic dyes from aqueous solutions, Environ. Technol. Innov. 17 (2020) 100612.
[25] Z. Guan, J. Lv, P. Bai, X. Guo, Boron removal from aqueous solutions by adsorption—a review, Desalination 383 (2016) 29–37.
[26] M.A. Al-Ghouti, D.A. Da'ana, Guidelines for the use and interpretation of adsorption isotherm models: a review, J. Hazard Mater. 393 (2020) 122383.
[27] V. Masindi, M.W. Gitari, H. Tutu, M. Debeer, Removal of boron from aqueous solution using magnesite and bentonite clay composite, Desalin. Water Treat. 57 (44) (2016) 20957–20969.
[28] D. Kavak, Removal of boron from aqueous solutions by batch adsorption on calcined alunite using experimental design, J. Hazard Mater. 163 (2009) 308–314.
[29] H. Demey, T. Vincent, M. Ruiz, A.M. Sastre, E. Guibal, Development of a new chitosan/Ni(OH)2-based sorbent for boron removal, Chem. Eng. J. 244 (2014) 576–586.
[30] E.A. Bursalı, Y. Seki, S. Seyhan, M. Delener, M. Yurdakoç, Synthesis of chitosan beads as boron sorbents, J. Appl. Polym. Sci. 122 (2011) 657–665.
[31] M. Ruiz, C. Tobalina, H. Demey-Cedeño, J.A. Barron-Zambrano, A.M. Sastre, Sorption of boron on calcium alginate gel beads, React. Funct. Polym. 73 (2013) 653–657.
[32] Y.K. Recepoglu, N. Kabay, I. Yilmaz-Ipek, M. Arda, M. Yuksel, K. Yoshizuka, S. Nishihama, Deboronation of geothermal water using N-methyl-D-glucamine based chelating resins and a novel fiber adsorbent: batch and column studies, J. Chem. Technol. Biotechnol. 92 (2017) 1540–1547.
[33] S. Bhagyaraj, M.A. Al-Ghouti, P. Kasak, I. Krupa, An updated review on boron removal from water through adsorption processes, Emergent Mater 1–20 (2021).
[34] Q. Luo, L. He, X. Wang, H. Huang, X. Wang, S. Sang, X. Huang, Cyclodextrin derivatives used for the separation of boron and the removal of organic pollutants, Sci. Total Environ. 749 (2020) 141487.
[35] A. Melliti, J. Kheriji, H. Bessaies, B. Hamrouni, Boron removal from water by adsorption onto activated carbon prepared from palm bark: kinetic, isotherms, optimisation and breakthrough curves modeling, Water Sci. Technol. 81 (2) (2020) 321–332.
[36] L.K. Li, S.N.A.M. Jamil, L.C. Abdullah, N.N.L.N. Ibrahim, A.A. Adekanmi, M. Nourouzi, Application of feed-forward and recurrent neural network in modelling the adsorption of boron by amidoxime-modified poly(Acrylonitrile-co-Acrylic Acid), Environ. Eng. Res. 25 (6) (2020) 830–840.
[37] S. Bai, J. Han, C. Du, J. Li, W. Ding, Removal of boron and silicon by a modified resin and their competitive adsorption mechanisms, Environ. Sci. Pollut. Res. 27 (24) (2020) 30275–30284.

Sara A. Wahib, Dana A. Da'na, Mohammad Y. Ashfaq, Mohammad A. Al-Ghouti*
Department of Biological and Environmental Sciences, College of Arts and Sciences, Qatar University, Doha, P.O. Box: 2713, Qatar

* Corresponding author.
E-mail address: mohammad.alghouti@qu.edu.qa (M.A. Al-Ghouti).